ADVANCED THERAPEUTICS
www.advtherap.com

A Nanoparticle Platform for Improved Potency, Stability, and Adjuvanticity of Poly(I:C)

*Emily C. Gale, Gillie A. Roth, Anton A. A. Smith, Marcela Alcántara-Hernández, Juliana Idoyaga, and Eric A. Appel**

Cancer immunotherapies and prophylactic vaccines against infectious diseases often exploit adjuvants such as toll-like receptor agonists (TLRa) to drive potent and directed immune responses. Unfortunately, a promising class of TLRa based on nucleic acid derivatives is susceptible to degradation by nucleases, cause life-threatening systemic toxicities, and is difficult to target to specific cell populations or tissues within the body. In this study a library of cationic polymeric nanoparticles (NP) is developed for encapsulation and delivery of the double-stranded RNA structural mimic, poly(I:C) (pIC), to address these limitations. Using a combinatorial library screening approach, pIC/poly(β-amino ester) (PBAE) NPs are identified that skew activation resulting in enhanced potency (13-fold increase in type I interferon [IFN] production) and negligible toxicity. These highly potent adjuvant NPs increase the magnitude, duration, and affinity maturation of antigen-specific antibodies following vaccination with a model subunit vaccine. This NP platform provides an opportunity to alter the immune response to pIC, creating a potent type I IFN-producing adjuvant capable of driving stronger humoral responses to immunization and improving affinity maturation more than 14-fold. This platform can be applied generally to develop more effective vaccines and immunotherapies.

Despite a global rise in immunization rates in recent decades, 1.5 million deaths occur each year from vaccine-preventable diseases.[1] Subunit vaccines are safe and scalable but are less immunogenic than whole pathogen vaccines.[2] The development of potent and stable adjuvants is necessary to increase the immunogenicity of subunit vaccines to increase their efficacy and to reduce the spread of infectious diseases.[3] The double-stranded RNA mimic, poly(I:C) (pIC), activates both endosomal and cytosolic receptors and is one of the strongest type I Interferon (IFN) producers, elevating both humoral- and cell-mediated responses to specific antigens (**Figure 1**A).[4] Unfortunately, life-threatening toxicity, rapid degradation both in vitro and in vivo, and difficulty in controlling biodistribution have prevented translation of pIC beyond early-stage clinical trials.[5,6] A complex of pIC with poly-L-lysine and carboxymethylcellulose (pICLC), which exhibits reduced rates of hydrolysis and reduced thermal denaturation compared to pIC, is the most clinically advanced pIC analogue.[7] However, pICLC is no more potent than pIC and results in similar levels of cytokine production.[8] Liposomes and microspheres have also been considered for pIC delivery, but typically require complex and/or poorly scalable syntheses.[6] Here, we establish a simple method for encapsulation of pIC to improve stability, passively target pIC to lymph nodes, and promote uptake by professional antigen presenting cells (APCs), including dendritic cells (DCs) to ultimately increase type I IFN production.[9] In this work, we sought to address limitations of pIC delivery by utilizing cationic poly(β-amino ester) (PBAE) polymers to encapsulate pIC into nanoparticles (NPs).[10] PBAEs have been successfully used to deliver an array of other nucleic acids such as DNA, siRNA, and

E. C. Gale, G. A. Roth, Dr. A. A. A. Smith, Prof. E. A. Appel
Department of Materials Science and Engineering
Stanford University
Stanford, CA 94305, USA
E-mail: eappel@stanford.edu
E. C. Gale
Department of Biochemistry
Stanford University School of Medicine
Stanford, CA 94305, USA
G. A. Roth, Prof. E. A. Appel
Department of Bioengineering
Stanford University
Stanford, CA 94305, USA
Dr. M. Alcántara-Hernández, Prof. J. Idoyaga
Department of Microbiology and Immunology
Stanford University School of Medicine
Stanford, CA 94305, USA
Dr. M. Alcántara-Hernández
Program in Immunology
Stanford University School of Medicine
Stanford, CA 94305, USA
Prof. J. Idoyaga, Prof. E. A. Appel
Institute for Immunity
Transplantation and Infection
Stanford University School of Medicine
Stanford, CA 94305, USA
The ORCID identification number(s) for the author(s) of this article can be found under https://doi.org/10.1002/adtp.201900174

DOI: 10.1002/adtp.201900174

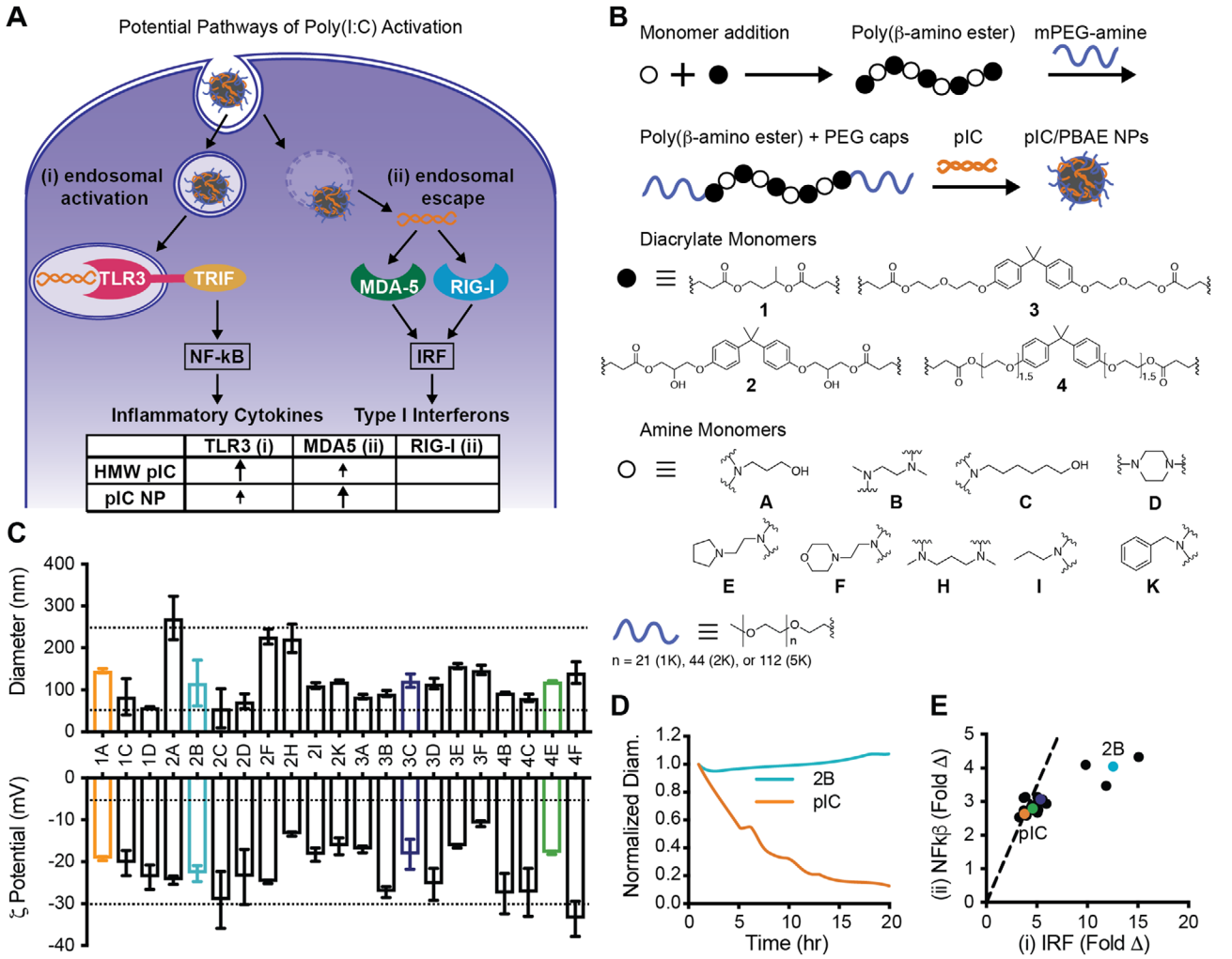

Figure 1. Encapsulation of pIC in PBAE NPs alters and enhances immune activation. A) Pathways activated by soluble pIC or NPs. pIC can activate TLR3 in endosomes (i) and can escape endosomes to activate RLR receptors (ii), MDA-5, and RIG-I. The table shows predicted activation of the different pathways based on literature.[12] Activation of RLR receptors leads to more efficient type I IFN production. B) NP synthesis schematic. PBAE polymers generated from the monomer libraries shown were mixed with pIC at a 1:1 weight ratio to form coacervate NPs. C) NP hydrodynamic diameters and surface zeta potentials of NPs in water ($n = 3$). D) Stability of pIC or pIC/PBAE NPs over time during continuous agitation under physiological conditions in the presence of RNAse (1 μM). E) Relative in vitro NF$\kappa\beta$/IRF activation ratio of different pIC/PBAE NP formulations compared to soluble pIC. Activation was determined by A549-Dual Reporter Cell assay following 24 h incubation with 3 μg mL^{-1} pIC. Data depict mean ± SD.

mRNA to increase stability and potency.[11,12] In previous studies of DNA and RNA delivery, tuning PBAE chemistry (e.g., hydrophobicity, charge density, and H-bonding capacity), and NP size was shown to provide a large screening space to optimize potency and specificity.[10] Here, we characterize and screen a library of pIC/PBAE NPs (Figure 1B) for increased potency and reduced toxicity and assess the in vivo efficacy of pIC/PBAE NPs in a model subunit vaccine. We identified a formulation that increased type I IFN production 13-fold compared to pIC alone in vivo, and dramatically enhanced the magnitude, duration, and affinity maturation of antigen-specific antibodies following vaccination.

PIC can activate endosomal toll-like receptor 3 (TLR3) and cytosolic retinoic acid-inducible gene I-like (RIG-I-like) receptors (RLRs), melanoma differentiation-associated protein 5 (MDA-5) and RIG-I.[13] After endocytosis, pIC either remains in the endosome (Figure 1A,i) or is transported into the cytosol (Figure 1A,ii) to activate strong type I IFN-producing RLRs.[13,14] We aimed to engineer pIC encapsulation technology in a manner that increased type I IFN production, which is correlated with potent and durable anti-viral and anti-cancer immunity.[13] We hypothesized that delivery of pIC in certain PBAE NPs could enhance endosomal escape and therefore activation of the cytosolic RLR pathways, increasing potency and specificity of type I IFN production.

In this study we screened a combinatorial library of PBAE polymers capped with polyethylene glycol (PEG). Polymers were characterized by gel permeation chromatography (GPC) and ^{1}H NMR (Table S1 and Figures S2–S4, Supporting Information). Number-average molecular weights (M_n) ranged from 2–6 kDa (Table S1, Supporting Information). Complexation of anionic pIC and cationic

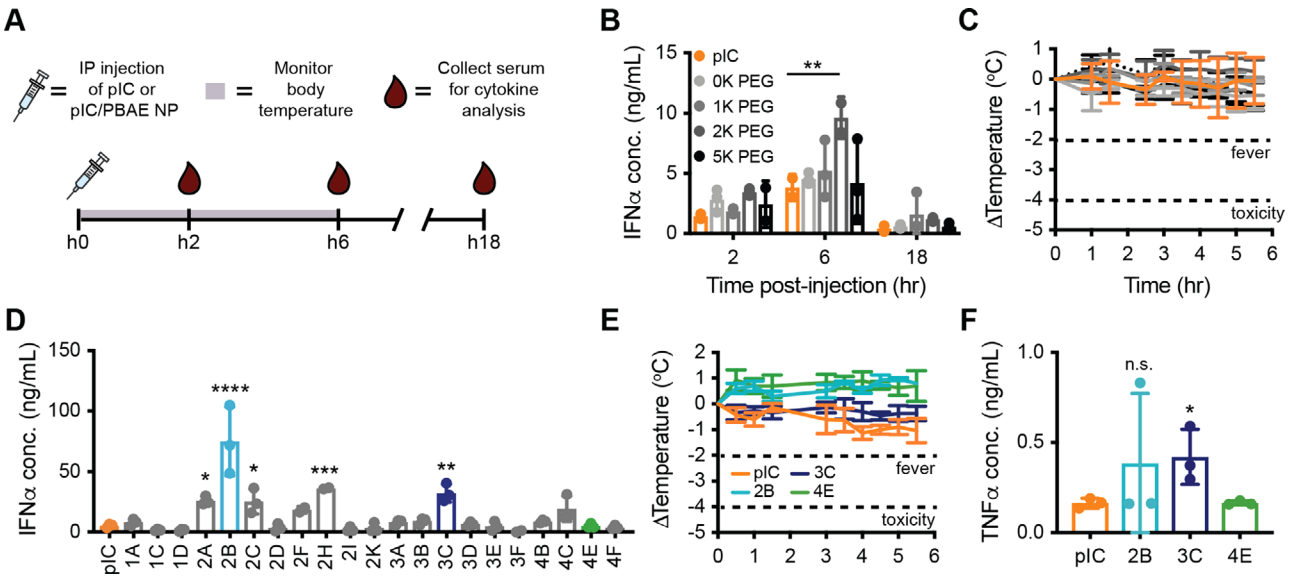

Figure 2. pIC/PBAE NPs boost IFNα production without increasing toxicity. A) Timeline for in vivo IFNα and toxicity study. 50 µg pIC either soluble or in pIC/PBAE NPs was administered i.p. Temperature was monitored for 6 h and serum was collected at 2, 6, and 18 h. B) ELISA analysis of IFNα in serum at 2, 6, and 18 h following administration of NPs made from monomers 1 and A (from Figure 1B) with different length mPEG-amine caps (0–5 K) (n = 3). C) Change in mouse body temperature following NP administration, where a decrease >2 °C indicates fever and >4 °C indicates toxicity (n = 3; colors correspond to those in part B). D) ELISA analysis of IFNα in serum 6 h after treatment (n = 3). E) Change in mouse body temperature following select treatments (n = 3). F) Concentration of serum TNFα 2 h after injection (n = 3). Data depict mean ± SD; values were analyzed by ordinary one-way ANOVA with multiple comparisons. *p < 0.05, **p < 0.01, ***p < 0.001, ****p < 0.0001, n.s., not significant.

PBAE polymers formed NPs with diameters between 50 and 250 nm and slightly negative surface charges (Figure 1C and Table S1, Supporting Information). Based on literature reports, we hypothesized that these properties would reduce protein opsonization and aggregation while promoting lymph node trafficking and APC uptake.[15] Stability experiments at physiological conditions verified that the hydrodynamic diameter of the most potent PEG-coated pIC/PBAE NP (2B) remained stable over 20 h while soluble pIC reduced in size, likely due to degradation (Figure 1D and Figure S5, Supporting Information).[16] NP stability is crucial because hydrodynamic size impacts NP draining and biodistribution. Additionally, we hypothesize that minimal pIC degradation occurs in NP 2B during the 20 h since RNAse-driven degradation leads to further negative charges on the polyphosphate backbone, altering both the molecular weight and charge balance, and thus destabilizing the pIC/PBAE NPs. We then used A549-Dual Reporter Cells (InvivoGen) to quantify activation of transcription factors including IFN regulatory factor (IRF) and nuclear factor κB (NF-κB). These studies indicated that several NPs, including 2B (light blue), dramatically skewed activation toward the preferred RLR pathways and increased potency compared to soluble pIC (orange) alone (Figure 1E).

We also conducted an in vivo screen to identify the most activating, nontoxic pIC/PBAE NPs (**Figure 2**A). We initially tested pIC/PBAE NPs made from polymer 1A, based on the success of a similar polymer for gene delivery in previous reports,[10] with mPEG end-cappers of different molecular weights. We found that 2 kDa mPEG led to the greatest IFNα production and negligible change in body temperature, which is a measure of toxicity (Figure 2B,C). We hypothesize that the addition of 2 kDa mPEG end-groups leads to the formation of a hydrophilic corona around the NP that prevents aggregation, while still allowing uptake by immune cells.[15,17] Next, we screened a combinatorial library of PBAE polymers synthesized from different monomers while maintaining the same 2 kDa mPEG end-caps. PBAE NP 2B exhibited a 13-fold increase in serum IFNα compared to soluble pIC alone 6 h after intraperitoneal (i.p.) administration (Figure 2D). Polymer 2B alone led to minimal serum IFNα production compared to pIC/PBAE NP 2B and soluble pIC (Figure S6A,C, Supporting Information), indicating that the encapsulation of pIC into PBAE NP 2B drives the observed response. Interestingly, NP 2B administered subcutaneously (s.c.) exhibited over a 1000-fold decrease in serum IFNα levels, suggesting that pIC is acting locally rather than systemically when administered s.c. (Figure S6B, Supporting Information). We observed negligible changes in body temperature and minimal pro-inflammatory cytokine (TNFα) production across all groups tested, suggesting PBAE NPs did not cause excessive inflammation or tissue injury (Figure 2E,F and Figure S7A–C, Supporting Information). In summary, we identified an encapsulation technology for pIC that skews activation toward the desired cytosolic RLR pathway and dramatically increased type I IFN production, while exhibiting negligible toxicity.

To investigate whether pIC/PBAE NPs enhanced the humoral immune response to a model ovalbumin (OVA) vaccine, we vaccinated mice s.c. with OVA antigen and either soluble pIC or select pIC/PBAE NPs (2B, 3C, or 4E). On day 33, mice received the same vaccine as a boost. We collected serum over time and measured both antibody concentration and affinity for OVA antigen (**Figure 3**A). Mice vaccinated with PBAE NP 2B produced significantly higher concentrations of serum IgG1 anti-OVA antibodies prior to the vaccine boost than those vaccinated

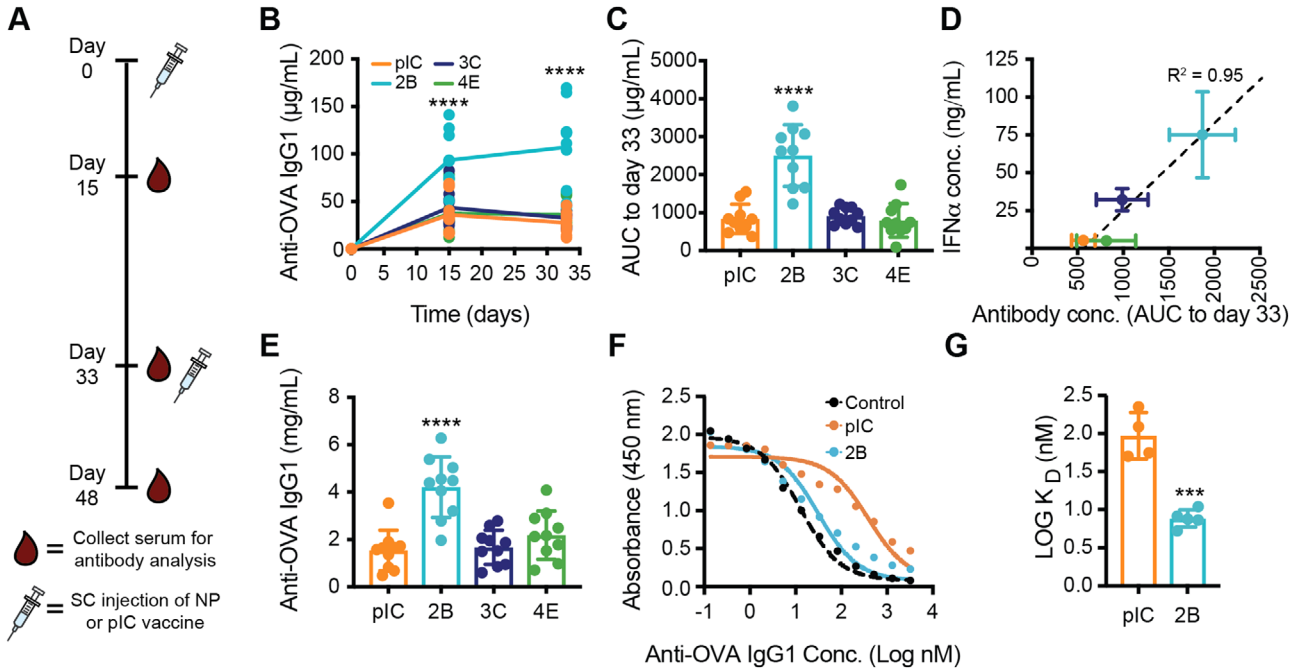

Figure 3. Potent pIC/PBAE NPs enhance humoral immunity and affinity maturation. A) Timeline for vaccine study. Mice received an s.c. injection of 100 μg OVA and 50 μg pIC either soluble or in a pIC/PBAE NP on day 0 and on day 33. B) Anti-OVA IgG1 antibody concentration pre-boost. C) Area under the anti-OVA IgG1 curve (Figure 3B) until day 33. D) Correlation between IgG1 antibodies over time and IFNα production in vivo (values from Figure 2D). E) Anti-OVA IgG1 antibody concentration 15 days after the vaccine boost. F) Average binding curves for NP 2B or soluble pIC vaccine groups post-boost (day 48) compared to a mAb control (model and raw data shown in Figure S9A–C, Supporting Information). G) Calculated K_D values from fitted binding curves in (F). Data are mean ± SD; $n = 5$–10 per group (B,C,E). Data are mean ± SD; $n = 4$–5 per group (F,G). Values were analyzed by t test compared to pIC control at each timepoint (B). Values were analyzed by ordinary one-way ANOVA with multiple comparisons (C,E). Values were analyzed by t test. ***$p < 0.001$, ****$p < 0.0001$ (G).

with soluble pIC (Figure 3B,C). We observed a strong correlation between in vivo IFNα production and anti-OVA antibody production following vaccination, consistent with reports highlighting the importance of type I IFNs for activation of the downstream adaptive immune response to a target antigen (Figure 3D).[8] Following the vaccine boost, IgG1 antibody levels in all groups increased dramatically and antibody concentration remained comparatively higher for mice that received PBAE NP 2B rather than soluble pIC (Figure 3E). There was no significant difference in IgG2c antibody production or the ratio of IgG1 to IgG2c antibodies between groups, suggesting that there was a negligible difference in the level of class switching and only a minor shift toward a T helper cell type 2 (Th2) response for PBAE NP 2B when compared with soluble pIC (Figure S8A,B, Supporting Information). Critically, the ability to neutralize pathogens upon infection depends on both antibody concentration and the affinity for antigen.[18] For this reason, it is notable that the affinity of antibodies for OVA antigen following prime-boost vaccination was 14-fold higher in mice that received PBAE NP 2B compared to those that received soluble pIC (Figure 3F,G and Figure S9, Supporting Information). These results indicate that the enhanced primary antibody response to vaccines comprising PBAE NP 2B led to greater affinity maturation and thus higher quality immunity compared to vaccines comprising soluble pIC.

Nucleic acid toll-like receptor agonists (TLRa), including pIC and CpG ODN, have shown incredible promise as adjuvants in prophylactic vaccines and cancer immunotherapies.[19–21] pIC is a potent type I IFN producer that induces strong cell-based and humoral immunity, but has not progressed clinically due to limitations of stability, delivery, and toxicity.[8] Type I IFNs are also believed to underlie favorable disease outcomes following immunotherapy in a range of cancers.[20] The pIC analogue pICLC, has progressed to phase II clinical trials, but has not been FDA approved.[21] While we did not directly compare pICLC to pIC/PBAE NPs in this study, previous reports indicate that pICLC and soluble pIC treatment exhibit comparable serum type I IFN levels in mice,[8] suggesting that the potent type I IFN-producing NPs described here would be more potent than pICLC in vivo. To increase clinical relevance of pIC, a delivery system must be developed that can reduce degradation, aid in targeting of specific cell types, and prevent systemic toxicity.[8] In this study we conducted a screen of pIC/PBAE NPs comprising distinct polymers and identified a nontoxic NP formulation that exhibited a 13-fold increase in type I IFN production in vivo when compared with soluble pIC. We demonstrate that encapsulation of pIC in PBAE NP 2B skews activation in vitro from TLR3 to MDA-5 and leads to both a 2.5-fold increase in antigen-specific antibody concentration and a 14-fold increase in antibody affinity after prime-boost vaccination in vivo. This NP platform provides an opportunity to enhance the immune response to nucleic acid adjuvants and could be applied to generate more effective delivery of diverse TLRa adjuvants such as CpG ODN. The development of next-generation subunit vaccines and cancer immunotherapies can potentially benefit from employing TLRa NPs such

as those described here that induce even greater type I IFN production.

Experimental Section

Poly(β-amino ester) Synthesis: A library of acrylate-terminated PBAEs was synthesized by mixing diacrylate and amine monomers at a 1:0.95 molar ratio (Figure 1B). Reactions were performed by mixing monomers in dioxane solution (600 mg mL^{-1}) with 20 mol% 1,8-diazobicylcoundecene (DBU) as a catalyst for 4 h at 90 °C while stirring. Backbone PBAE polymers were precipitated in 50 times reaction volume of diethyl ether followed by centrifugation at 8000 rpm for 1 min. Polymers were dried in a vacuum desiccator overnight. Subsequently, PBAE polymers were dissolved in anhydrous tetrahydrofuran (50 mg mL^{-1}) and combined with a 2.05 molar excess 1, 2, or 5 kDa methoxy-PEG amine to react while stirring overnight at room temperature. The final mPEG-capped polymers were precipitated in 50 times the reaction volume of hexanes followed by centrifugation at 8000 rpm for 1 min. After washing, polymers were dried in a vacuum desiccator. Polymer solutions were dissolved in DMSO (100 mg mL^{-1}) and stored at −20 °C.

Reporter Cell Line Assay: The A549-Dual cell line (InvivoGen, a549d-nfis) was used in this study. Cells were cultured at 37 °C with 5% CO_2 in DMEM (Thermo Fisher Scientific) supplemented with L-glutamine (2 mM), D-glucose (4.5 g L^{-1}), 10% heat inactivated fetal bovine serum (Atlanta Biologicals), and penicillin (100 U mL^{-1})/streptomycin (100 µg) (Gibco). Growth medium was supplemented with blasticidin (10 µg mL^{-1}) and zeocin (100 µg mL^{-1}) (InvivoGen). Soluble pIC or a pIC/PBAE NP solution (20 µL) was added to a 96-well tissue culture treated plate to a final pIC concentration of 3 µg mL^{-1}. About 50 000 cells were added to each well in 180 µL of media. Cells were cultured for 24 h at 37 °C in a CO_2 incubator before following manufacturer instructions for SEAP and luciferase quantification.

Animal Studies: 8–10-week-old female C57BL/6 mice were obtained from Charles River and were cared for according to Institutional Animal Care and Use guidelines. Animal studies were performed in accordance with the guidelines for the care and use of laboratory animals; all protocols were approved by the Stanford Institutional Animal Care and Use Committee.

In Vivo Cytokine Quantification: Mice were injected with buffer (100 µL) containing pIC HMW (50 µg) (InvivoGen) either in soluble form or encapsulated in NPs. Mice were injected i.p. since this administration route resulted in quantifiable cytokine levels across treatment groups. For polymer control experiments, polymer samples were prepared as NPs were, but were dropped into a solution that did not contain pIC (Supporting Information). Serum was collected at the indicated times by tail vein blood collection and stored at −80 °C. Serum cytokine concentrations (IFNα and TNFα) were determined by ELISA according to the manufacturer's instructions (PBL Assay Science and Thermo Fisher Scientific, respectively). Absorbance was measured at 450 nm in a Synergy H1 Microplate Reader (BioTek). Cytokine concentrations were calculated from the standard curves and represented as ng mL^{-1}.

Mouse Body Temperature Measurements: Mice were injected s.c. with Implantable Programmable Temperature Transponders (Bio Medic Data Systems). Experiments began 1 week after injection of the transponder to allow for complete wound healing. Mouse temperatures were recorded by scanning mice with a compatible Bio Medic Data Systems Smart Probe at 30 min intervals for 6 h and again at 18 h after receiving the treatment.

Vaccination Experiment: Mice received a s.c. injection (125 µL) containing pIC (50 µg) either encapsulated in NPs or in soluble form and OVA (100 µg) in their backs under brief isoflurane anesthesia. Injections were done with a 26-gauge needle. Mouse blood was collected from the tail vein for survival studies or through cardiac puncture for terminal studies.

Antibody Concentration: Serum concentrations were measured using an anti-OVA mouse IgG1 ELISA (Cayman Chemicals). Serum was diluted 1:1000 in assay buffer for pre-boost samples and 1:100 000 for post-boost samples. The ELISA was performed according to the manufacturer's instructions. Plates were analyzed using a Synergy H1 Microplate Reader (BioTek Instruments) at 450 nm. Serum antibody concentrations were calculated from the standard curves represented as µg mL^{-1} or mg mL^{-1}.

Antibody Affinity: Twelve serial dilutions of serum were mixed with a constant concentration of HRP-conjugated anti-OVA antibody (3 nM) (BioLegend) and incubated in an OVA-coated plate for 2 h at room temperature. The wells were washed, incubated with TMB substrate, and the reaction was stopped with HCl (1 N). Absorbance was read with a plate reader at 450 nm. Data was fit with a one-site competitive binding model using Graphpad Prism. The control antibody was assumed to have a K_D of 1 nM based on common affinities of mAbs found in the industry. This assumption affects only the absolute K_D values reported and not the relative differences between treatment groups. Statistics were performed on the $\log_{10}(K_D)$ values.

Statistical Analysis: Data in Figure 1D data were normalized by initial diameter (Figure S5, Supporting Information) and data in Figure 1E were divided by solvent-only values to find the fold change for each IRF and NF$\kappa\beta$ activation. Data are presented as mean ± SD. $n = 3$ for groups in Figures 1C and 2B–F, $n = 5$–10 per group in Figure 3B,C,E, and $n = 4$–5 per group in Figure 3F,G. In Figure 2 values were analyzed by ordinary one-way ANOVA with multiple comparisons. In Figure 3C,E values were analyzed by ordinary one-way ANOVA with multiple comparisons and in Figure 2B,G values were analyzed by *t* test.*$p < 0.05$, **$p < 0.01$, ***$p < 0.001$, ****$p < 0.0001$, n.s., not significant. GraphPad Prism was used for statistical analysis.

Supporting Information

Supporting Information is available from the Wiley Online Library or from the author.

Acknowledgements

E.C.G. would like to thank members of the Appel lab for their useful discussion and advice throughout this project. This research was financially supported by the Center for Human Systems Immunology with Bill and Melinda Gates Foundation (OPP1113682). E.C.G. is grateful for the NIH-funded Cell and Molecular Biology Training Program (T32 GM007276).

Conflict of Interest

The authors declare no conflict of interest.

Keywords

adjuvants, immunoengineering, nanoparticles, polymers, vaccines

Received: September 11, 2019
Revised: October 15, 2019
Published online:

[1] R. M. Casey, L. Dumolard, C. Danovaro-Holliday, M. Gacic-Dobo, M. S. Diallo, L. M. Hampton, A. S. Wallace, *Morb. Mortal. Wkly. Rep.* **2016**, *65*, 1270.
[2] M. Black, A. Trent, M. Tirrell, C. Olive, *Expert Rev. Vaccines* **2010**, *9*, 157.
[3] S. Singha, K. Shao, K. K. Ellestad, Y. Yang, P. Santamaria, *ACS Nano* **2018**, *12*, 10621.
[4] S. Barbuto, J. Idoyaga, M. Vila-Perello, M. P. Longhi, G. Breton, R. M. Steinman, T. W. Muir, *Nat. Chem. Biol.* **2013**, *9*, 250.

[5] M. R. Rosenfeld, M. C. Chamberlain, S. A. Grossman, D. M. Peereboom, G. J. Lesser, T. T. Batchelor, S. Desideri, A. M. Salazar, X. Ye, *Neuro-Oncology* **2010**, *12*, 1071.
[6] A. M. Hafner, B. Corthésy, H. P. Merkle, *Adv. Drug Delivery Rev.* **2013**, *65*, 1386.
[7] M. Saxena, R. L. Sabado, M. La Mar, H. Mohri, A. M. Salazar, H. Dong, J. Correa Da Rosa, M. Markowitz, N. Bhardwaj, E. Miller, *Front. Immunol.* **2019**, *10*, 4937.
[8] M. P. Longhi, C. Trumpfheller, J. Idoyaga, M. Caskey, I. Matos, C. Kluger, A. M. Salazar, M. Colonna, R. M. Steinman, *J. Exp. Med.* **2009**, *206*, 1589.
[9] L. M. Kranz, M. Diken, H. Haas, S. Kreiter, C. Loquai, K. C. Reuter, M. Meng, D. Fritz, F. Vascotto, H. Hefesha, C. Grunwitz, M. Vormehr, Y. Husemann, A. Selmi, A. N. Kuhn, J. Buck, E. Derhovanessian, R. Rae, S. Attig, J. Diekmann, R. A. Jabulowsky, S. Heesch, P. Langguth, S. Grabbe, C. Huber, O. Tureci, U. Sahin, *Nature* **2016**, *534*, 396.
[10] D. G. Anderson, A. Akinc, N. Hossain, R. Langer, *Mol. Ther.* **2005**, *11*, 426.
[11] K. L. Kozielski, S. Y. Tzeng, J. J. Green, *Chem. Commun.* **2013**, *49*, 5319.
[12] H. Lopez-Bertoni, K. Kozielski, Y. Rui, B. Lal, H. Vaughan, D. Wilson, N. Mihelson, C. Eberhart, J. Laterra, J. J. Green, *Nano Lett.* **2018**.
[13] L. Gitlin, W. Barchet, S. Gilfillan, M. Cella, B. Beutler, R. A. Flavell, M. S. Diamond, M. Colonna, *Proc. Natl. Acad. Sci. U. S. A.* **2006**, *103*, 8459.
[14] T. A. Nguyen, B. R. C. Smith, M. D. Tate, G. T. Belz, M. H. Barrios, K. D. Elgass, A. S. Weisman, P. J. Baker, S. P. Preston, L. Whitehead, A. Garnham, R. J. Lundie, G. K. Smyth, M. Pellegrini, M. O'Keeffe, I. P. Wicks, S. L. Masters, C. P. Hunter, K. C. Pang, *Immunity* **2017**, *47*, 498.
[15] E. J. Chaney, L. Tang, R. Tong, J. Cheng, S. A. Boppart, *Mol. Imaging* **2010**, *9*, 153.
[16] P. Mastorakos, E. Song, C. Zhang, S. Berry, H. W. Park, Y. E. Kim, J. S. Park, S. Lee, J. S. Suk, J. Hanes, *Small* **2016**, *12*, 678.
[17] R. Gref, Y. Minamitake, M. T. Peracchia, V. Trubetskoy, V. Torchilin, R. Langer, *Science* **1994**, *263*, 1600.
[18] L. Hangartner, R. M. Zinkernagel, H. Hengartner, *Nat. Rev. Immunol.* **2006**, *6*, 231.
[19] S. P. Kasturi, I. Skountzou, R. A. Albrecht, D. Koutsonanos, T. Hua, H. I. Nakaya, R. Ravindran, S. Stewart, M. Alam, M. Kwissa, F. Villinger, N. Murthy, J. Steel, J. Jacob, R. J. Hogan, A. Garcia-Sastre, R. Compans, B. Pulendran, *Nature* **2011**, *470*, 543.
[20] L. Zitvogel, L. Galluzzi, O. Kepp, M. J. Smyth, G. Kroemer, *Nat. Rev. Immunol.* **2015**, *15*, 405.
[21] B. Temizoz, E. Kuroda, K. J. Ishii, *Int. Immunol.* **2016**, *28*, 329.